

Mitigation Techniques of Channel Collisions in the TTFR-Based Asynchronous Spectral Phase-Encoded Optical CDMA System

Takaya Miyazawa and Iwao Sasase

Abstract: In this paper, we propose a chip-level detection and a spectral-slice scheme for the tunable-transmitter/fixed-receiver (TTFR)-based asynchronous spectral phase-encoded optical code-division multiple-access (CDMA) system combined with time-encoding. The chip-level detection can enhance the tolerance of multiple access interference (MAI) because the channel collision does not occur as long as there is at least one weighted position without MAI. Moreover, the spectral-slice scheme can reduce the interference probability because the MAI with the different frequency has no adverse effects on the channel collision rate. As a result, these techniques mitigate channel collisions. We analyze the channel collision rate theoretically, and show that the proposed system can achieve a lower channel collision rate in comparison to both conventional systems with and without the time-encoding method.

Index Terms: Channel collision, multiple access interference (MAI), optical CDMA, spectral phase-encoding, tunable-transmitter/fixed-receiver (TTFR).

I. INTRODUCTION

Conventional optical local access networks typically use wavelength-division multiplexing (WDM) or time-division multiplexing (TDM) techniques which require wavelength and time domain processing. Recently, optical code-division multiple-access (OCDMA) is gaining attention, due to its potential for enhanced information security, simple and decentralized network control, as well as enhanced flexibility in the granularity of the provisioned bandwidth. In OCDMA networks, different user signals may overlap both in time and frequency domains in a common communication medium; multiple-access is achieved by assigning different, minimally interfering code sequences to different transceiver pairs. Instead of relying on fixed WDM or TDM channel assignment, OCDMA can utilize optical codes to achieve truly flexible access of large network capacity.

As an encoding/decoding scheme in the OCDMA systems, the spectral phase-encoding has demonstrated strong potentials to achieve high-performance coherent OCDMA communica-

tions by using femtosecond pulses [1]–[6]. The spectral phase-encoding scheme assigns a pseudo-random bipolar code sequence to each user, and determines Fourier transform of the transmitted pulse for a given user by encoding phases in the transmitted spectrum according to the assigned code sequence. There is another encoding method which is spectral-amplitude-encoding [7]. The encoding method assigns a pseudo-random code sequence to each user as in the spectral-phase-encoding. But, the spectral-amplitude-encoding scheme transmits only wavelengths corresponding to the code “1” and does not transmit the wavelengths corresponding to the code “0.” The authors in [8] show that the spectral-phase-encoding is superior to the spectral-amplitude-encoding in terms of BER performances due to the higher processing gain. Thus, in this paper, we focus on the spectral-phase-encoding. Generally, the spectral phase-encoded OCDMA systems suffer from multiple access interference (MAI) of other active users. As the number of active users increases, the system performance degrades because of the increased MAI.

In an OCDMA network based on a passive star-coupler, multiple end nodes share the optical bandwidth by using OCDMA codes. Each node includes a transceiver for data transmission and detection by encoding or decoding messages using the correct code. This paper mainly focuses on a tunable-transmitter and fixed-receiver (TTFR) scheme as the nodal architecture. In the TTFR-based system, each receiver receives a unique bipolar code sequence assignment and the encoder in the transmitter tunes to the code sequence of the decoder in the receiver [2], [3], [9]. The TTFR achieves simpler system configurations and protocols because the receiver employs only one fixed decoder without requiring a centralized control for code assignment, and is suitable for optical local access networks which require low-cost system construction. Besides, from a viewpoint of physical layer, the TTFR-based system has the advantage that a receiver can obtain multiple access signals at the same time as long as the photo detection occurs at different time for different signals. However, in the TTFR-based system, multiple users may employ the same frequency-domain code sequence to send data to the same destination receiver. Therefore, a *channel collision* occurs and all simultaneous packets to the same destination will fail because a receiver cannot individually detect the multiple colliding signals [2]. Here, in [2], the *channel collision* is defined as the status where two or more packets transmitted to the same destination receiver overlap each other. But, from a viewpoint of physical layer, a receiver can receive multiple packets simultaneously as long as the detection timings of peak-outputs are different among the packets. Thus, in this paper, we define

Manuscript received August 20, 2007; approved for publication by G. Hugh Song, Division I Editor, December 10, 2007.

This work is partly supported by Grant-in-Aid for Scientific Research of the Ministry of Education, Culture, Sports, Science and Technology (MEXT) and the Japan Society for the Promotion of Science (JSPS), the Foundation of Ando Laboratory, and the Grant in the Global Center of Excellence Program “High-Level Global Cooperation for Leading-Edge Platform on Access Spaces” of Keio University from MEXT, Japan.

T. Miyazawa is with the National Institute of Information and Communications Technology (NICT), email: takaya@nict.go.jp.

I. Sasase is with the Department of Information and Computer Science, Keio University, email: sasase@ics.keio.ac.jp.

the *channel collision* as the status where the detection timings coincide among the multiple access signals and an abnormally high peak-value detection occurs at the receiver. By detecting the channel collision, the receiver recognizes that the photo-detection timings overlap among multiple access users' signals. Channel collisions in the TTFR-based system leads to achieve nulling of "code spreading gain in the frequency domain" which is defined as how many interference pulses are tolerated in the decoder. Thus, we must mitigate channel collisions by obtaining the code spreading gain in another domain (e.g., *time domain*).

Previous studies [5] investigated a combination of spectral phase-encoding and time-encoding, in which the effect of optical beat noise is neglected. The application of the time-encoding has an advantageous effect that the code spreading gain in the time domain increases, which improves the system performance when the code spreading gain in the frequency domain can be sufficiently obtained. However, it has an adverse effect that the interference probability in the time domain increases. Especially the TTFR-based system suffers from the adverse effect. This is because the code spreading gain in the frequency domain cannot be obtained in the case of channel collision, and thus, the average noise components significantly increase by applying the time-encoding. As a result, only the addition of time-encoding results in degradation of the channel collision rate in the TTFR-based spectral phase-encoded OCDMA system. Thus, we require schemes to reduce the channel collision rate.

In this paper, we propose a *chip-level detection* and a *spectral-slice scheme* for the TTFR-based asynchronous spectral phase-encoded OCDMA system combined with time-encoding. The chip-level detection can enhance the tolerance of the MAI because channel collisions do not occur so long as there is at least one weighted time position without MAI in a bit-time. Moreover, the spectral-slice scheme can reduce the interference probability because MAI pulses at the different frequencies have no adverse effects on the channel collision rate. In other words, the proposed schemes mitigate the channel collision by taking advantage of the fact that the phase-decoded pulses spread out in time domain through the time-encoding. As a result, these techniques can reduce the channel collision rate compared to the conventional systems. We analyze the channel collision rate theoretically by applying a Gaussian approximation to the avalanche photo-diode (APD) output [6], [11], and show that the proposed system can achieve a lower channel collision rate in comparison to both conventional systems with and without the time-encoding method.

II. SYSTEM DESCRIPTION

Fig. 1 illustrates an OCDMA network based on a passive star coupler. In this broadcast-and-select network, all inputs from various nodes are combined in the passive star coupler and the mixed optical signal is broadcasted to all users. As we described in Section I, we focus on the TTFR-based nodal architecture. Here, the N -bit M-sequence code is employed as a set of "frequency-domain" code sequences where $N (= 2^k - 1, k: \text{positive integer})$ is the code-length [2], [5], [6]. Each receiver is assigned a unique M-sequence code. We employ on-off-keying

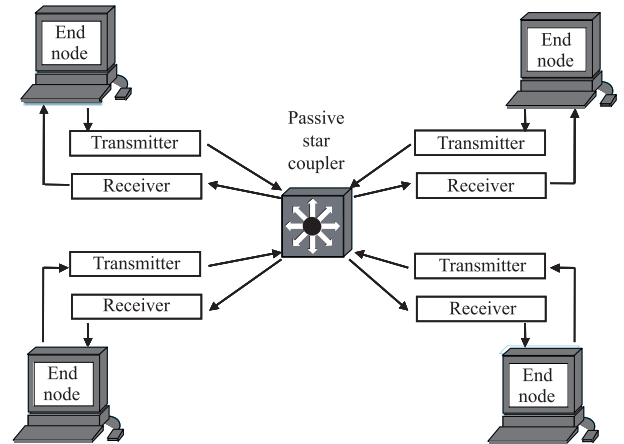


Fig. 1. The network model.

(OOK) as a modulation scheme, in which a pulse or no pulse is transmitted in accordance with bit information "1" or "0," respectively. Pulse-position modulation (PPM) is another major modulation scheme [6]. Our proposed schemes are effective also in the system using PPM. But, in this study, we focus on the OOK in order to clarify fundamental improvement factors of the proposed schemes. We assume an asynchronous transmission system in which a frame (i.e., a bit time) is asynchronous among multiple users.

A. Conventional Schemes

In this study, we let the width of the detection time of the APD (i.e., "chip") be much shorter than a bit-time (i.e., "frame").

Fig. 2 shows an example of transmitted pulses and the decoding processes in the conventional spectral phase-encoded OCDMA system without the time-encoding. In this example, all users employ the same M-sequence code to send data to the same destination receiver. In the systems, the detector employs two kinds of thresholds. One is for the OOK decoder and is set to the intensity of a phase-decoded pulse for a single user. The other is for channel collision detection and is twice as high as the threshold value for OOK decoding. We label these thresholds as *1st-threshold* and *2nd-threshold*, respectively. As illustrated in this example, the channel collision occurs when multiple access signals encoded by the same code simultaneously arrive at the receiver.

Fig. 3 shows an example of transmitted pulses and the decoding processes in the conventional spectral phase-encoded OCDMA scheme with only time-encoding. The scheme employs the (F, ω) -optical orthogonal code (OOC), whose out-of-phase autocorrelation and maximum cross-correlation value are bounded by one, as a set of "time-domain" code sequences [10]. " F " is the code length and " ω " is the number of weights. Each transmitter randomly selects a (F, ω) -OOC out of all OOCs. We also assume that the transmissions among users are bit(frame)-asynchronous, but chip-synchronous since the performance in the chip-synchronous case results in the upper bound on the performance of the frame-asynchronous system [9], [11]. In this example, the abnormally high peak-value exceeding the *2nd-threshold* is detected in the receiver for User 1, indicating chan-

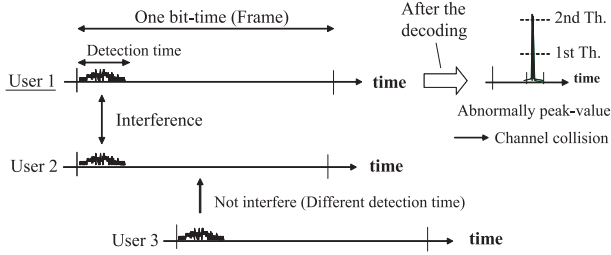


Fig. 2. An example of transmitted pulses and the decoding in the conventional scheme without time-encoding.

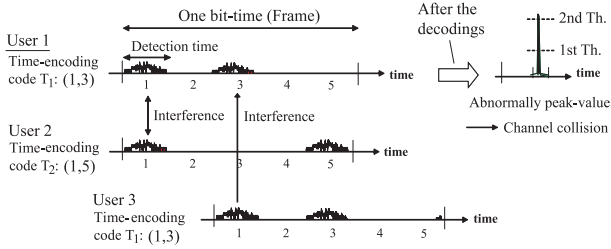


Fig. 3. An example of transmitted pulses and the decoding methods in the conventional scheme with only time-encoding.

nel collision. As we explained in Introduction, the increase of the interference probability due to the time-encoding causes a significant increase of noise power in the receiver on average. This scheme experiences higher channel collision rates.

B. Proposed Spectral Phase-Encoded OCDMA Scheme With Time-Encoding, Spectral-Slice and Chip-Level Detection

This section describes the transmitter and receiver structures in the proposed system, and also explains an example of the transmitted pulses and the decoding methods.

B.1 The System Structure

Fig. 4 shows the block diagram of the transmitter in the proposed system. The frequency band of a launched optical pulse is divided into two bands and each band is phase-encoded by using the same M-sequence code. After that, the phase-encoded pulses in the first and second bands are embedded into the chip-time positions corresponding to the first and second elements in the OOC (i.e., weighted time positions), respectively. As an example, if the weighted positions of the OOC are 1st and 3rd, the phase-encoded pulses in the first and second bands are embedded into the 1st and 3rd positions, respectively. Note that the value of ω can be increased though the value of code-length in each frequency band should equal to or be larger than the maximum number of active users. In this paper, we assume that the system divides the frequency bandwidth into two areas (i.e., $\omega = 2$) to clarify the fundamental improvement factor of the proposed scheme compared with the conventional schemes. We can easily expect that the higher value of ω results in an increased improvement factor.

Fig. 5 shows the block diagram of the receiver in the proposed system. The received pulses are phase-decoded in each frequency bandwidth to generate peak values. The received signals are detected by the chip-level detection instead of the cor-

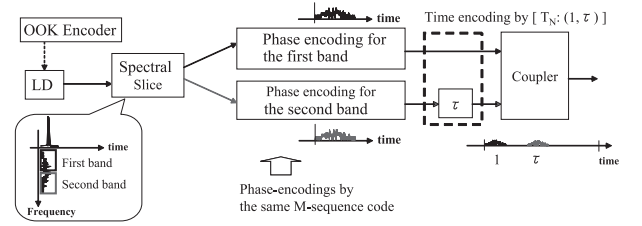


Fig. 4. The block diagram of the transmitter in the proposed system.

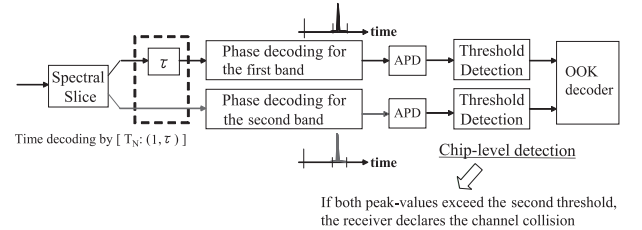


Fig. 5. The block diagram of the receiver in the proposed system.

relator. The chip-level detection is a technique used in the time-encoding OCDMA system to mitigate the effect of MAI [12]. In the chip-level detection, the threshold detections are applied separately in each peak-value. The chip-level detection has a good advantage that a large amount of MAI interfering with some weighed time positions do not affect on the system performance as long as there is at least one weighted time position without MAI in a frame [12].

The spectral slicing is the same technique as the WDM. But, the novelty of our proposal is that the system sends two pulses encoded by the same M-sequence with separate wavelength bands on the separate weighted positions of OOC. Similar techniques called bipolar-unipolar code and electronic hard-limiters/regenerators have been proposed in [18]. Our work is different from the one in [18] as below: The scheme in [18] encodes the pulses by using separate M-sequences at the same wavelength band in the weighted positions of OOC, and therefore imperatively requires an ultra-fast optical switch in the receiver, which is too complicated and difficult to be implemented. On the other hand, our proposed scheme encodes the pulses by using the same M-sequence at the separate wavelength bands in the weighted positions of OOC, and therefore does not require the ultra-fast optical switch in the receiver. In addition, the authors in [18] have proposed the electronic hard-limiters/regenerators. These techniques are equipped to eliminate the noise components which arise from the desired signal in a weighted position in the process of decoding by other M-sequences except the desired M-sequence, and thus, are totally different from our chip-level detection in principle. Our chip-level detection is a MAI mitigation technique and is equipped to correctly decide received bits when at least one weighted position receives no MAI pulses. Moreover, in our proposed system, only frequency-domain code-sequence (i.e., M-sequence) is uniquely assigned to each receiver. However, if the scheme in [18] is applied to the TFR-based optical CDMA system, a combination of frequency-domain code-sequence and time-domain code-sequence (i.e., a wavelength-time codeword)

needs to be assigned to each receiver. Then, in the system using the scheme in [18], when the starting positions of frames overlap among two signals which are sent to the same destination (i.e., encoded by the same code-sequence), all weighted positions simultaneously overlap among the signals and the channel collision inevitably occurs. This means that, in the TFR-based optical CDMA system, the channel collision rate of the scheme in [18] equals to that of the conventional scheme without the time-encoding. On the other hand, our proposed scheme can reduce the channel collision rate by using the chip-level detection and spectral-slice scheme.

In addition, the proposed system encodes the two pulses by using an M-sequence with the shorter (i.e., half) code-length after the spectral slicing process. In doing so, we keep the total wavelength bandwidth to send one bit constant among the conventional and proposed systems. This means that the proposed scheme does not cause the spectral expansion.

Here, a frame is asynchronous among users, but needs to be synchronized between the transmitter and the receiver before the actual data transmission because the receiver needs to recognize the source transmitter and the timings of threshold detection to the peak values. Therefore, the transmitter sends the training bit sequence consisting of a string of “1”s to the receiver in advance of actual data transmission. And, when a detected peak value in the first band exceeds the *1st-threshold*, the receiver looks into the time position of the peak value in the second band in order to know the detection timing positions (i.e., the weighted positions of the OOC). Detecting only one peak value which exceeds the *1st-threshold* in the second band, the receiver knows the OOC. When both APD outputs in the first and the second bands have abnormally high peak-values exceeding the “2nd”-threshold, the receiver recognizes that channel collision is occurring. Then, the receiver tells the transmitter to stop the data transmission as soon as channel collision is detected. If more than two peak outputs are detected in a frame, the receiver cannot find which OOC the desired user is using. In that case, the receiver individually demodulates the data information corresponding to all combinations of the OOCs obtained from the peak outputs. For example, if the peak output in the first band is detected in the 1st weighted position and the peak outputs in the second band are detected in the 3rd and 4th weighted positions, the receiver individually demodulates the data corresponding to (1, 3) and (1, 4). The receiver recognizes the existence of MAI pulses when errors are detected by looking into error detection bits such as Frame check sequence in the process of actual data packet transmission. The proposed spectral-slice scheme makes the synchronization processing easier because the receiver can recognize the starting position of frame (i.e., bit time) by the existence of peak-value in the first band. This is one of the advantages of the proposed system.

B.2 An Example of Transmitted Pulses

Fig. 6 shows an example of transmitted pulses and the decoding methods in the proposed system. The interference patterns are the same as in Fig. 3, but User 4 is active. We regard the User 1 as the desired user, and the User 2, User 3, and User 4 as the other active users. In this example, the interference pulses with the first band from User 2 and User 4 hit the 1st chip

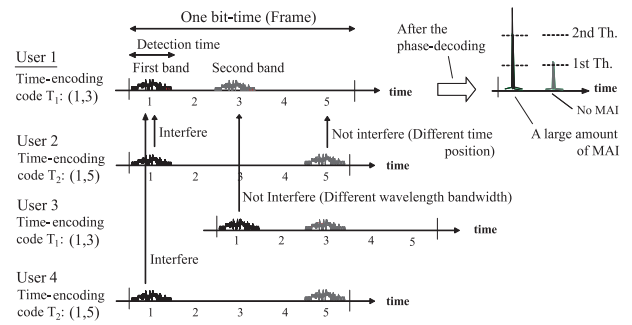


Fig. 6. An example of transmitted pulses and the decoding methods in the proposed scheme.

time position of User 1. Therefore, the phase-decoded pulse in the 1st chip time position of User 1 drastically exceeds the 2nd-threshold. On the other hand, the interference with the first band from User 3 hits the 3rd chip time position of User 1, but it has no effect on the phase-decoded pulse because the 3rd chip time position of User 1 detects only pulses with the second band. In addition, the pulses with the second band from User 2, User 3 and User 4 do not hit the 3rd chip time position of User 1 and has no adverse effect on the phase-decoded pulse. As a result, since the peak value in the 3rd chip time position of User 1 does not exceed the 2nd-threshold, the chip-level detector can recognize the abnormally high peak-value in the 1st chip-time position as the one caused from the MAI. Thus, in this example, the spectral slice scheme and the chip-level detection can avoid channel collision even though the first weighted time-position of User 1 receives a large amount of MAI. This means that the proposed scheme can reduce the channel collision rate compared to both conventional schemes with and without the time-encoding.

III. THEORETICAL ANALYSIS

We define channel collision rate (CCR) as the probability that the detection timings coincide among the multiple access signals and abnormally high peak-value detections exceeding the 2nd-threshold occur at the receiver. This section theoretically analyzes the CCR of the proposed system.

The systems do not perform the channel collision detection in the process of actual data transmission (i.e., sending “1” or “0” by OOK), but perform it in the process of synchronization between the transmitter and receiver (i.e., sending the training bit sequence consisting of a string of “1”s). The transmitter and receiver need to be synchronized in advance of the actual data transmission. This means that the proposed system certainly sends a bit “1” when the channel collision detection is performed, and after that, sends actual data information consisting of “1” and “0.” This is why we set the threshold of the channel collision detection (i.e., 2nd threshold) to two and the threshold of the OOK decoder (i.e., 1st threshold) to one.

In the process of channel collision detection, there is a possibility of the miss detection that a receiver detects the received signal of which the intensity is less than the 2nd threshold in spite of having collisions from two simultaneous transmitters. When the miss detection occurs, the receiver cannot detect the channel collision. Thus, the miss detection affects the bit error

rate in the process of actual data transmissions. We analyze and evaluate the rate of miss detection in addition to the CCR in this paper.

We denote the total number of active users by N . We classify the other active users into following classes;

1. With the same M-sequence code (i.e., the same destination) and the same OOC as the desired user's codes.
2. With the same M-sequence code and the different OOC.
3. With the different M-sequence code and the same OOC.
4. With the different M-sequence code and the different OOC.

We denote the number of each user class by N_{ss} , N_{sd} , N_{ds} , and N_{dd} , respectively. This means that $N = N_{ss} + N_{sd} + N_{ds} + N_{dd} + 1$ where "1" corresponds to the desired user. We denote the number of the M-sequence codes (i.e., the code length) by N_f , the maximum number of active users (i.e., the number of subscribers) by N_{\max} . Note that $N \leq N_{\max} \leq N_f$. We also denote the detection (response) time in the APD and one bit-time by T_D (ps) and R_r (ps), respectively. Then, the bit-rate per user, R_b (Gbps)=1000/ R_r , and the code-length for OOC, F , is expressed as R_r/T_D . When we denote the number of weights for OOC by ω , the number of available OOC, $N_t \leq (F - 1)/(\omega(\omega - 1))$ [10]. In addition, we denote the received optical powers belonging to a single user in a bit-time before and after amplification in the receiver by P_{be} and P_{af} , respectively. In this paper, we consider the MAI, the thermal noise, the shot noise in the APD, the noises in the optical amplifier, and the optical beat interference as contributors to the performance deterioration.

The occurrence probability of the above four kinds of other users (i.e., $[ss]$ - $[dd]$ users), $\Pr(\text{users})$, is a multinomial distribution expressed as

$$\Pr(\text{users}) = \frac{(N-1)!}{N_{ss}!N_{sd}!N_{ds}!N_{dd}!} \alpha_{ss}^{N_{ss}} \alpha_{sd}^{N_{sd}} \alpha_{ds}^{N_{ds}} \alpha_{dd}^{N_{dd}} \quad (1)$$

where α_{xy} ($x \in (s, d), y \in (s, d)$) is expressed as

$$\begin{aligned} \alpha_{ss} &= (1/N_f)(1/N_t), \\ \alpha_{sd} &= (1/N_f)(1 - 1/N_t), \\ \alpha_{ds} &= (1 - 1/N_f)(1/N_t), \\ \alpha_{dd} &= (1 - 1/N_f)(1 - 1/N_t). \end{aligned} \quad (2)$$

Next, we analyze the occurrence probability of interference from the four kinds of users. In a weighted chip-time position in the proposed scheme, the MAI at the different frequencies has no adverse effects on the channel collision rate. In addition, in this study, we clarify the probability that the channel collision occurs when the desired user sends the training bit sequence, and thus we can assume that the desired user sends only "1". But, in our analysis, we assume that the other active users send actual data consisting of both "1" and "0" because the actual data bit sequence is much longer than the training bit sequence. When any one of other users sends a pulse, the system can recognize the channel collision by detecting the abnormally high peak-value. But, since other users send data by OOK modulation, the interference probability from any one of other users is expressed as $1/2F$ regardless of the user type (i.e., $[ss]$, $[sd]$, $[ds]$ or $[dd]$), where "1/2" indicates that the other user sends "1"

or "0." It is probable that the MAI from a $[ss]$ or a $[ds]$ user hits both weighted chip-time positions of the desired user at the same time. When the interference with the first band from the $[ss]$ and the $[ds]$ users hits the former weighted chip-time position, the interference with the second band from the users also hits the latter weighted chip-time position at the same time. We denote the numbers of the $[ss]$ and the $[ds]$ users which interfere by p_{ss} and p_{ds} , respectively. On the other hand, the MAI from a $[sd]$ or a $[dd]$ user occurs at most one weighted position owing to the cross-correlation property of OOC. p_{sd} and p_{dd} represent the numbers of the $[sd]$ and the $[dd]$ users which hit the former chip-time position of the desired user, respectively. We also denote the numbers of the $[sd]$ and the $[dd]$ users which hit the latter chip-time position of the desired user by q_{sd} and q_{dd} , respectively. Then, the occurrence probability of interference from the four kinds of other user, $\Pr(\text{Interference})$, is expressed as

$$\begin{aligned} \Pr(\text{Interference}) &= \\ &\binom{N_{ss}}{p_{ss}} \left(\frac{1}{2F}\right)^{p_{ss}} \left(1 - \frac{1}{2F}\right)^{q_{ss}} \\ &\cdot \binom{N_{sd}}{p_{sd}} \binom{N_{sd} - p_{sd}}{q_{sd}} \left(\frac{1}{2F}\right)^{p_{sd} + q_{sd}} \left(1 - \frac{2}{2F}\right)^{r_{sd}} \\ &\cdot \binom{N_{ds}}{p_{ds}} \left(\frac{1}{2F}\right)^{p_{ds}} \left(1 - \frac{1}{2F}\right)^{q_{ds}} \\ &\cdot \binom{N_{dd}}{p_{dd}} \binom{N_{dd} - p_{dd}}{q_{dd}} \left(\frac{1}{2F}\right)^{p_{dd} + q_{dd}} \left(1 - \frac{2}{2F}\right)^{r_{dd}} \end{aligned} \quad (3)$$

where $r_{sd} = N_{sd} - p_{sd} - q_{sd}$ and $r_{dd} = N_{dd} - p_{dd} - q_{dd}$. $q_{ss} = N_{ss} - p_{ss}$ and $q_{ds} = N_{ds} - p_{ds}$.

In the system, the receiver learns of the *channel collision* when it detects abnormally high peak-values exceeding the 2nd-threshold in both weighted time-positions. We denote the 1st-threshold value by θ , and then the 2nd-threshold value is set to 2θ . We denote the probabilities that the APD outputs in the former and the latter weighted positions (frequencies), Y_f and Y_l , exceed 2θ by $\Pr(Y_f \geq 2\theta)$ and $\Pr(Y_l \geq 2\theta)$, respectively. According to [20], it is known that the probabilities can be expressed by the complementary error function, $\text{erfc}(\cdot)$, and are shown as

$$\Pr(Y_\zeta \geq 2\theta) = \frac{1}{2} \text{erfc} \left(\frac{2\theta - \mu_\zeta}{\sqrt{2}\sigma_\zeta} \right) \quad (4)$$

where $\zeta \in (f, l)$, and $\text{erfc}(\cdot)$ is expressed as

$$\text{erfc}(z) = \frac{2}{\sqrt{\pi}} \int_z^\infty \exp(-u^2) du \quad (5)$$

μ_ζ and σ_ζ^2 are the mean value and the variance of the APD output, respectively. They are expressed as [6]

$$\begin{aligned} \mu_\zeta &= G(\alpha(P_{af}/\omega + z_{\zeta s} + z_{\zeta d}) + I_d), \\ \sigma_\zeta^2 &= G^2 \alpha^2 (z_{\zeta s} + z_{\zeta d})^2 \\ &\quad + (e(\alpha(P_{af}/\omega + z_{\zeta s} + z_{\zeta d}) + I_d)G^{2+ex} + \sigma_{th}^2) B_e \\ &\quad + (\sigma_s^2 + \sigma_{sig-sp-\zeta}^2 + \sigma_{sp-sp}^2) + \sigma_{beat-\zeta}^2 \end{aligned} \quad (6)$$

where α is $e\eta/hf_r$ [6]. e is the electron charge, η is the APD quantum efficiency, h is the Planck's constant, and f_r is the optical frequency. G is the APD gain, I_d is the dark current, ex is

$$\Pr(CCR) = \sum_{N_{ss}=0}^{N-1} \sum_{N_{sd}=0}^{N-1-N_{ss}} \sum_{N_{ds}=0}^{N-1-N_{ss}-N_{sd}} \sum_{p_{ss}=0}^{N_{ss}} \sum_{p_{sd}=0}^{N_{sd}} \sum_{q_{ds}=0}^{N_{sd}-p_{sd}} \sum_{p_{ds}=0}^{N_{ds}} \sum_{p_{dd}=0}^{N_{dd}} \sum_{q_{dd}=0}^{N_{dd}-p_{dd}} \Pr(Y_f \geq 2\theta) \Pr(Y_l \geq 2\theta) \Pr(\text{users}) \Pr(\text{Interference}). \quad (12)$$

$$\Pr(MD) = \sum_{N_{ss}=0}^{N-1} \sum_{N_{sd}=0}^{N-1-N_{ss}} \sum_{N_{ds}=0}^{N-1-N_{ss}-N_{sd}} \sum_{p_{ss}=0}^{N_{ss}} \sum_{p_{sd}=0}^{N_{sd}} \sum_{q_{ds}=0}^{N_{sd}-p_{sd}} \sum_{p_{ds}=0}^{N_{ds}} \sum_{p_{dd}=0}^{N_{dd}} \sum_{q_{dd}=0}^{N_{dd}-p_{dd}} \left(\Pr((Y_f < 2\theta) \cap (Y_l \geq 2\theta) \mid ((p_{ss} + p_{sd}) \geq 1) \cap ((p_{ss} + q_{sd}) \geq 1)) \right. \\ \left. + \Pr((Y_f \geq 2\theta) \cap (Y_l < 2\theta) \mid ((p_{ss} + p_{sd}) \geq 1) \cap ((p_{ss} + q_{sd}) \geq 1)) \right. \\ \left. + \Pr((Y_f < 2\theta) \cap (Y_l < 2\theta) \mid ((p_{ss} + p_{sd}) \geq 1) \cap ((p_{ss} + q_{sd}) \geq 1)) \right) \Pr(\text{users}) \Pr(\text{Interference}). \quad (13)$$

the excess noise factor, B_e is the electrical bandwidth, and σ_{th}^2 is the variance of thermal noise [6]. z_{ζ_s} and z_{ζ_d} ($\zeta \in (f, l)$) are MAI powers expressed as

$$\begin{aligned} z_{fs} &= (p_{ss} + p_{sd})P_{af}, \\ z_{fd} &= (p_{ds} + p_{dd})P_{af}/N_f, \\ z_{ls} &= (p_{ss} + q_{sd})P_{af}, \\ z_{ld} &= (p_{ds} + q_{dd})P_{af}/N_f. \end{aligned} \quad (7)$$

σ_s^2 , $\sigma_{sig-sp-\zeta}^2$, and σ_{sp-sp}^2 are the shot noise, the signal-ASE (amplified spontaneous emission) noise, and the ASE-ASE noise due to the optical amplification, respectively, which are expressed as [15]

$$\begin{aligned} \sigma_s^2 &= 2eG_2\alpha P_{be}B_e, \\ \sigma_{sig-sp-\zeta}^2 &= 2e\eta G_2^2 F_n \alpha (P_{be} + (z_{\zeta_s} + z_{\zeta_d})/10^{0.1G_2})B_e, \\ \sigma_{sp-sp}^2 &= e^2\eta^2 G_2^2 F_n^2 \Delta\nu_{opt} B_e \end{aligned} \quad (8)$$

where $P_{be} = P_{af}/10^{0.1G_2}$. F_n is amplifier noise figure [15], and we set $F_n = 2$ which is the ideal value. G_2 is the optical amplifier gain, $\Delta\nu_{opt}$ is the optical bandwidth, T_D is the response time of APD, and T_C is the duration of a non-encoded original peak pulse. In this system, $B_e = 1/(T_D \cdot 10^{-12})$ and $\Delta\nu_{opt} = 1/(T_C \cdot 10^{-15})$.

$\sigma_{beat-\zeta}^2$ is optical beat interference which is expressed as

$$\sigma_{beat-\zeta}^2 = \sigma_{1-beat-\zeta}^2 + \sigma_{2-beat-\zeta}^2 \quad (9)$$

where $\sigma_{1-beat-\zeta}^2$ and $\sigma_{2-beat-\zeta}^2$ are the variances of the beat noise and the secondary beat noise, respectively, and expressed as [16]

$$\begin{aligned} \sigma_{1-beat-f}^2 &= 2(p_{ss} + p_{sd} + p_{ds} + p_{dd})\xi_f(G\alpha P_{af})^2, \\ \sigma_{2-beat-f}^2 &= (p_{ss} + p_{sd} + p_{ds} + p_{dd}) \\ &\quad \cdot (p_{ss} + p_{sd} + p_{ds} + p_{dd} - 1)\xi_f^2(G\alpha P_{af})^2, \\ \sigma_{1-beat-l}^2 &= 2(p_{ss} + q_{sd} + p_{ds} + q_{dd})\xi_l(G\alpha P_{af})^2, \\ \sigma_{2-beat-l}^2 &= (p_{ss} + q_{sd} + p_{ds} + q_{dd}) \\ &\quad \cdot (p_{ss} + q_{sd} + p_{ds} + q_{dd} - 1)\xi_l^2(G\alpha P_{af})^2 \end{aligned} \quad (10)$$

Table 1. Link parameters.

Symbol	Meaning	Value
T_c	duration of ultrashort pulse	80 fsec
f_r	optical frequency	1.934×10^{14} Hz
η	APD quantum efficiency	0.75
e	electron charge	1.602×10^{-19} C
G	APD gain	300
ex	excess noise factor	0.35
i_d	dark current	1.0×10^{-10} A
k_B	Boltzmann's constant	1.38×10^{-23} W/K · Hz
T_r	receiver temperature	1100°K
R_L	load resistance	1030Ω
G_2	optical amplifier gain	50 dB
T_D	detection time of the APD	10 psec
N_{max}	maximum number of users	31

where ξ_ζ ($\zeta \in (f, l)$) is crosstalk level [16], which is expressed as $\xi_f = \langle P_{i,f} \rangle / P_d$ and $\xi_l = \langle P_{i,l} \rangle / P_d$, respectively. $\langle P_{i,\zeta} \rangle$ is the ensemble average of noise power and P_d is the desired user's signal power in a bit-time, and expressed as

$$\begin{aligned} \langle P_{i,f} \rangle &= \left(\frac{p_{ss} + p_{sd} + (p_{ds} + p_{dd})/N_f}{p_{ss} + p_{sd} + p_{ds} + p_{dd}} \right) P_{af}, \\ \langle P_{i,l} \rangle &= \left(\frac{p_{ss} + q_{sd} + (p_{ds} + q_{dd})/N_f}{p_{ss} + q_{sd} + p_{ds} + q_{dd}} \right) P_{af}, \\ P_d &= P_{af}. \end{aligned} \quad (11)$$

Then, we can obtain the channel collision rate in the proposed scheme, $\Pr(CCR)$, expressed as (12). Also, we can obtain the rate of miss detection in the proposed scheme, $\Pr(MD)$, expressed as (13).

IV. NUMERICAL RESULTS

Table 1 shows the link parameters in the systems. We define the received optical power as the power belonging to a single user arriving at the receiver (before the amplification) when the user sends a pulse, which equals to P_{be} . This study utilizes the same APD parameters as the ones in [6].

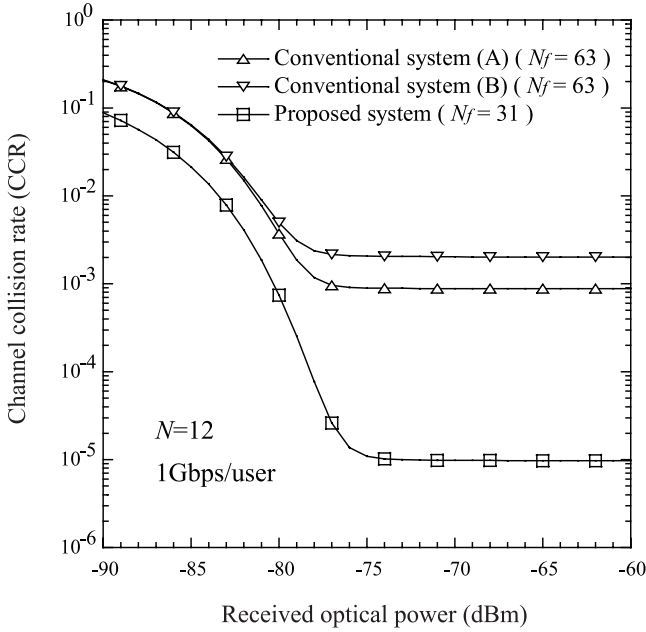


Fig. 7. Received optical power before amplification (P_{be}) versus CCR where $R_b = 1$ Gbps.

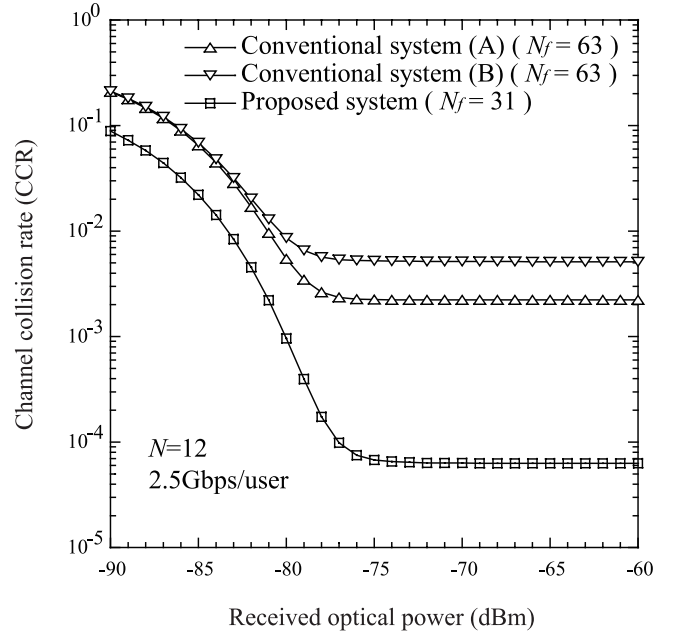


Fig. 8. Received optical power before amplification (P_{be}) versus CCR where $R_b = 2.5$ Gbps.

We do not consider the performances of XTTR ($X=“T”$ or $“F”$)-based systems but consider the ones of only TTFR-based systems because this paper focuses on CCR improvement effect of the proposed schemes in the TTFR-based systems. We compare the channel collision rate of the proposed system with those of the two conventional systems. The first conventional system is the one without the time-encoding labeled ‘Conventional system (A).’ The second conventional system is the one with only time-encoding labeled ‘Conventional system (B).’

Figs. 7 and 8 show the received optical power before amplification, P_{be} , CCR where the bit-rate per user, $R_b = 1$ Gbps and 2.5 Gbps, respectively. We set the response time of PD (T_D) to the chip-period (i.e., 10 ps). We assume that, in advance of the optical-electrical conversion in the APD, the systems employ optical time-gating [19] in order to eliminate the MAI components existing outside the time-duration of a non-encoded original peak pulse. (Currently, the time-gating is picosecond order, but will be femtosecond order along with the evolution of optical devices in the future, and thus, we assume that the system can perform the time-gating over a non-encoded original peak pulse.) In that case, the systems can distinguish the desired signal from the other signals encoded by different code sequences, and thus, the response time of PD does not need to be much smaller than the chip-period and can be set to the same value as the chip-period (i.e., 10 ps). (Recently, the response time of 10 ps has been achieved [13], [14].) Please note that 80 fs non-encoded original peak pulse is spectrally phase-encoded by M-sequence. In this study, since we set the code-length to 63 for the conventional systems and $31 \times (2 \text{ bands})$ for the proposed systems, the spectral phase-encoded pulse becomes $80 \text{ fs} \times 63 = 5.04 \text{ ps}$ which is around half of the chip-period (i.e., 10 ps). Thus, the probabilities that the two encoded pulses overlap within the response time (i.e., 10 ps) is large and the systems suffer from the effects of MAI and noises. In the case of $R_b = 1$

Gbps, one bit-time, $R_r = 1000/R_b = 1$ ns, and this means that the code length of OOC, F , equals 100. In the case of $R_b = 2.5$ Gbps, F equals 40. We assume $N = 12$ which means approximately 40% of all subscribers are active. Since the proposed scheme applies the spectral-slice scheme, the code-length for the M-sequence code (i.e., $N_f = 31$) is almost half as long as the one in the conventional schemes (i.e., $N_f = 63$). We can see that the proposed system can obtain lower channel collision rates compared to the conventional systems in any value of P_{be} . Generally, the longer code-length achieves better performance in the XTTR-based system due to the higher code spreading gain in frequency domain [6]. However, the TTFR-based system cannot obtain the code spreading gain in frequency-domain when the signals from multiple access users with the same frequency code sequence are mixed at the same time. This means that the longer code-length of M-sequence code does not have much effect on improvement of the performance in comparison to the shorter one. (Note that the value of code-length should be equal to or larger than the maximum number of active users which is 31 in this study.) The chip-level detection can enhance the tolerance of MAI, and the spectral-slice scheme can reduce the interference probability in the time-domain. Thus, the two techniques achieve mitigation of the channel collision in comparison with the conventional schemes. In addition, it can be seen that the floor of CCR is caused in the range of $P_{be} \geq -75$ dBm. It is because, even if the optical power is enough large to disregard the effect of noises arisen in the APD, the systems still suffer from the effects of MAI and optical beat interference which do not depend on the optical power. The proposed system individually detects each peak-value in the two weighted time-positions while the conventional systems collect the two peak pulses into the same time-position. This means that the proposed system requires around 3dB higher received optical power to achieve the

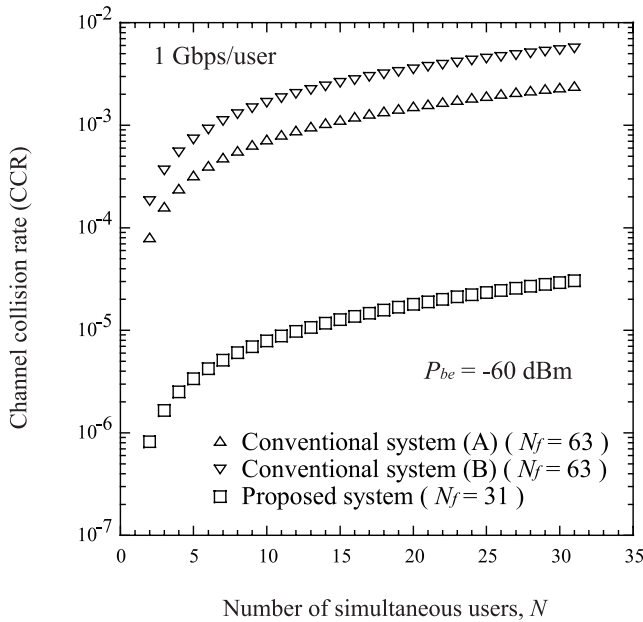


Fig. 9. Number of active users (N) versus CCR where $R_b = 1$ Gbps.

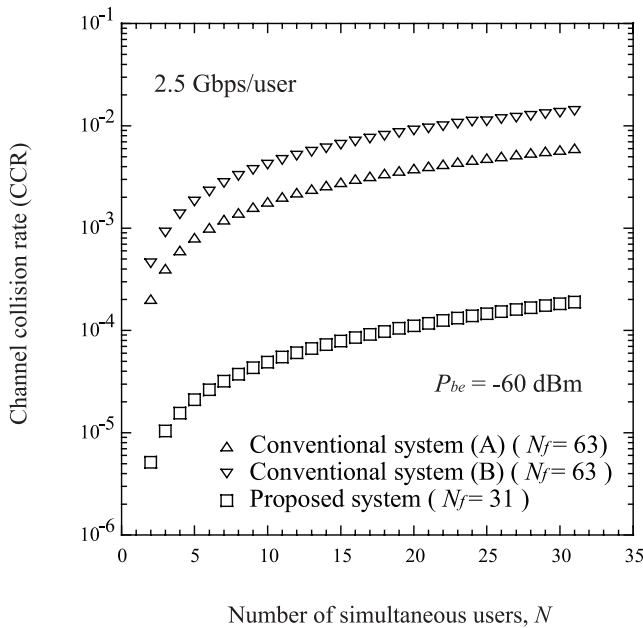


Fig. 10. Number of active users (N) versus CCR where $R_b = 2.5$ Gbps.

floor of CCR than the conventional systems under the condition that the optical power belonging to a single user in a bit-time is kept constant.

Figs. 9 and 10 show the number of active users, N , versus CCR where the bit-rate per user, $R_b = 1$ Gbps and 2.5 Gbps, respectively. We set $P_{be} = -60$ dBm in which every system achieves the floor of CCR in Figs. 7 and 8. We also set $N_f = 31$ for the proposed system, and $N_f = 63$ for the conventional systems. As Figs. 9 and 10 show, the proposed system can reduce the channel collision rate compared with the conventional systems in any value of N , due to the higher capacity for mitigation of the effect of MAI.

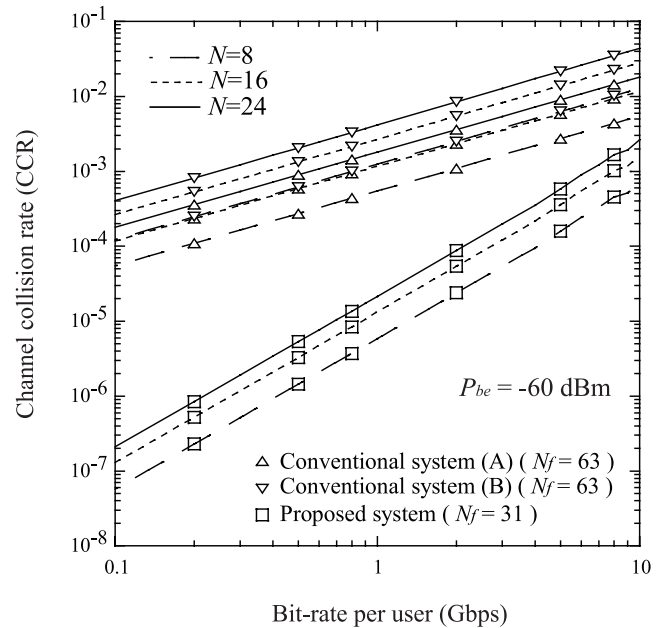


Fig. 11. Bit-rate per user (R_b) versus CCR where $N = 8, 16$, and 24.

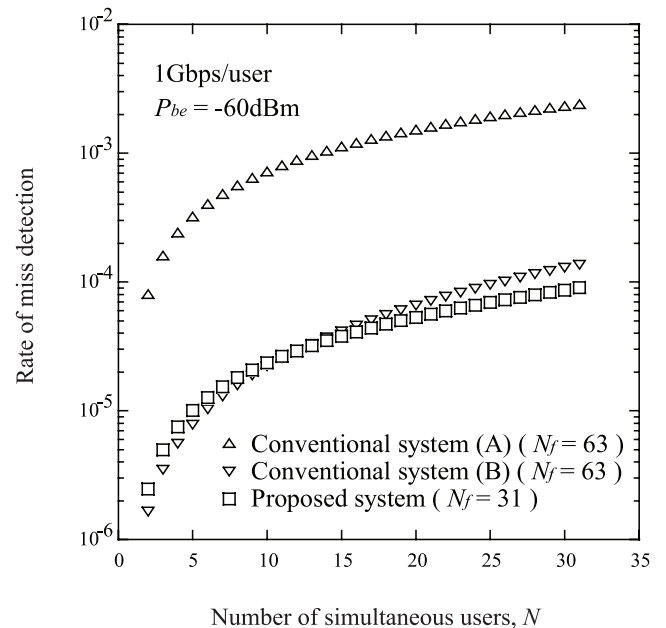


Fig. 12. Number of active users (N) versus rate of miss detection where $R_b = 1$ Gbps.

Fig. 11 shows bit-rate per user, R_b , versus CCR where $N = 8, 16$, and 24. This means that approximately 25%, 50%, and 75% of all subscribers are active, respectively. It can be seen that, as the value of R_b decreases, the channel collision rate decreases. This is because the decrease in the R_b value induces the increase in the F value, which in turn results in the decrease of the interference probability. In addition, we can see that the improvement effect of the proposed system increases as the value of R_b decreases. When the bit-rate is high, the system still suffers from multiple access interference even if the proposed schemes are applied because the value of F is too

small. In that case, it is not easy to mitigate the effect of MAI, and therefore the proposed system does not improve the channel collision so much. However, as the bit-rate becomes lower, the code-length of OOC becomes longer, and it is getting rare that the channel collision happens. In that case, the proposed system can easily and effectively mitigate the effect of MAI and increases the improvement factor of channel collision rate compared to the conventional systems.

Fig. 12 shows the number of simultaneous users versus rate of miss detection where $R_b = 1$ Gbps. We can see that the conventional system (B) has lower rate of miss detection than the conventional system (A). This is because the conventional system (B) can reduce the probability that the desired signal receives ω interference pulses in comparison to the conventional system (A), due to the higher code spreading gain in time domain. On the other hand, the proposed system has slightly higher rate of miss detection than the conventional system (B) when the number of simultaneous users is small. This is because, contrary to the conventional system (B), the proposed system does not collect the received pulses at the weighted positions, and thus is affected by noises more than the conventional system (B). However, when the number of simultaneous users is large, the proposed system can reduce the rate of miss detection, due to the capability for MAI mitigation of the chip-level detection and spectral-slice scheme.

Therefore, we can conclude that, in view of the two kinds of system performances (i.e., the CCR and the rate of miss detection), the proposed system is better than the two conventional systems.

Since each receiver is assigned a unique code-sequence in the TTFR-based optical CDMA system, the number of subscribers (i.e., maximum number of simultaneous users) equals to the number of code-sequences. (Please note that the number of available code-sequences of M-sequence equals to the code-length ($=2^n - 1$ (n : positive integer)).) Hence, the value of N_{max} cannot be set to more than 31 as long as the system employs the M-sequence of which the code-length is 31. Usually, we determine the code-length after assuming how many subscribers are accommodated (i.e., N_{max}) in the network. In this paper, we assume the optical CDMA network in which the number of subscribers (i.e., maximum number of simultaneous users) is 31, and thus set the code-length of M-sequence to 31. If we need to accommodate more number of subscribers, we must increase the code-length of M-sequence ($=2^n - 1$ (n : positive integer) employed in the system by increasing the value of n . The proposed scheme can reduce the channel collision rate in comparison to the conventional schemes regardless of the values of N_{max} and N_f , due to the capabilities for CCR reduction of the chip-level detection and spectral-slice scheme.

V. CONCLUSION

This paper proposed the chip-level detection and spectral-slice scheme for the TTFR-based asynchronous spectral phase-encoded OCDMA system combined with time-encoding. The chip-level detection can enhance the tolerance of MAI, while the spectral-slice scheme can reduce the interference probability in the time domain. As a result, these techniques can mit-

igate channel collisions. We analyze the channel collision rate theoretically, and show that the proposed system can achieve a lower channel collision rate in comparison to both conventional systems with and without the time-encoding.

ACKNOWLEDGMENTS

The authors would like to thank Prof. S. J. Ben Yoo, Prof. Zhi Ding and Dr. Fei Xue at University of California, Davis for their valuable comments and suggestions on this work.

REFERENCES

- [1] J. A. Salehi, A. M. Weiner, and J. P. Heritage, "Coherent ultrashort light pulse code-division multiple access communication systems," *J. Lightwave Technol.*, vol. 8, issue. 3, pp. 478–491, Mar. 1990.
- [2] F. Xue, Z. Ding and S. J. B. Yoo, "Performance analysis for optical CDMA networks with random access schemes," in *Proc. IEEE GLOBECOM 2004*, vol.3, pp. 1883–1887, Nov./Dec. 2004.
- [3] F. Xue, Z. Ding and S. J. B. Yoo, "Performance evaluation of optical CDMA networks with random media access schemes," in *Proc. IEEE Optical Fiber Communication Conference*, paper OThG5, Mar. 2005.
- [4] V. J. Hernandez, Y. Du, W. Cong, R. P. Scott, K. Li, J. P. Heritage, Z. Ding, B. H. Kolner and S. J. B. Yoo, "Spectral phase-encoded time-spreading (SPECTS) optical code-division multiple access for terabit optical access networks," *J. Lightwave Technol.*, vol. 22, no. 11, pp. 2671–2680, Nov. 2004.
- [5] T. Sonoda, K. Kamakura, T. Ohtsuki and I. Sasase, "Optical spread time CDMA systems combined with time domain OOC encoding," in *Proc. 1999 IEEE Pacific Rim Conference on Communications, Computers and Signal Processing (PACRIM'99)*, Aug. 1999, pp. 34–37.
- [6] K. Kamakura, T. Ohtsuki and I. Sasase, "Optical spread time CDMA communication systems with PPM signaling," *IEICE Trans. Commun.*, vol. E.82-B, no. 7, pp. 1038–1047, July 1999.
- [7] P. R. Prucnal, M. A. Santoro and T. R. Fan, "Spread spectrum fiber-optic local area network using optical processing," *J. Lightwave Technol.*, vol. LT-4, pp. 547–554, May 1986.
- [8] J. A. Salehi and C. A. Brackett, "Code division multiple-access techniques in optical fiber network -part I: Fundamental principles," *IEEE Trans. Commun.*, vol. 37, no. 8, pp. 824–833, Aug. 1989.
- [9] J. A. Salehi, "Code division multiple-access techniques in optical fiber network-part II: Systems performance analysis," *IEEE Trans. Commun.*, vol. 37, no. 8, pp. 834–842, Aug. 1989.
- [10] F. R. K. Chung, J. A. Salehi, and V. K. Wei, "Optical orthogonal codes: Design, analysis and applications," *IEEE Trans. Inf. Theory.*, vol. 35, pp. 595–604, May 1989.
- [11] H. M. Kwon, "Optical orthogonal code-division multiple access system-Part I: APD noise and thermal noise," *IEEE Trans. Commun.*, vol. 42, pp. 2470–2479, July 1994.
- [12] H. M. H. Shalaby, "Chip-level detection in optical code division multiple access," *J. Lightwave Technol.*, vol. 16, issue. 6, pp. 1077–1087, June 1998.
- [13] H. Ito, Y. Muramoto, T. Furuta, and Y. Hirota, "High-Speed and High-Output-Power Uni-Traveling-Carrier Photodiodes," in *Proc. the 18th Annual Meeting of the IEEE Lasers and Electro-Optics Society (LEOS 2005)*, Oct. 2005, pp. 456–457.
- [14] N. Kashio, K. Kurishima, K. Sano, M. Ida, N. Watanabe and H. Fukuyama, "Monolithic integration of InP HBTs and uni-traveling-carrier photodiodes using nonselective regrowth," *IEEE Trans. Electron Devices.*, vol. 54, no. 7, pp. 1651–1657, July 2007.
- [15] G. P. Agrawal, *Fiber-Optic Communication Systems*, 3rd Ed., Wiley-Interscience, 2002.
- [16] X. Wang, K. Kitayama, "Analysis of beat noise in coherent and incoherent time-spreading OCDMA," *J. Lightwave Technol.*, vol. 22, no. 10, pp. 2226–2235, Oct. 2004.
- [17] R. Papannareddy, A. M. Weiner, "Comparison of BER performance limits for coherent ultrashort light pulse and incoherent broadband CDMA systems," in *Proc. Conf. Lasers and Electro-Optics (CLEO)*, May 1999, pp. 330.
- [18] W. C. Kwong, G. C. Yang and Y. C. Liu, "A new family of wavelength-time optical CDMA codes utilizing programmable arrayed waveguide gratings," *IEEE J. Sel. Areas Commun.*, vol. 23, no. 8, Aug. 2005.

- [19] H. Sotobayashi, W. Chujo and K. Kitayama, "Highly spectral-efficient optical code-division multiplexing transmission system," *IEEE J. Sel. Topics in Quantum Electronics*, vol. 10, no. 2, pp. 250–258, March/April 2004.
- [20] R. M. Gagliardi and S. Karp, *Optical Communications*, 2nd Ed. JohnWiley & Sons, Inc., 1995.
- [21] A. D. McCoy, M. Ibsen, P. Horak, B. C. Thomsen, and D. J. Richardson, "Feasibility study of SOA-based noise suppression for spectral amplitude coded OCDMA," *J. Lightwave Technol.*, pp. 394–401, vol. 25, no. 1, Jan. 2007.



Takaya Miyazawa was born in Tokyo, Japan, on January 23, 1980. He received the B.E., M.E., and Ph.D. degrees in Information and Computer Science from Keio University, Yokohama, Japan, in 2002, 2004, and 2006, respectively. From 2006 to 2007, He was a post-doctoral fellow at Keio University. He was a visiting researcher of School of Information Technology and Engineering (SITE) at the University of Ottawa, Ottawa, ON, Canada, for two months in 2003 and Department of ECE at the University of California, Davis, CA, USA, for sixteen months in 2005–2006.

Now, he is affiliated with National Institute of Information and Communications Technology(NICT), Japan. He is engaged in researches on optical access network architecture, fiber-optic CDMA, optical-atmospheric CDMA, WDM and optical communication theory. He is a Recipient of the 2007 Hiroshi Ando Memorial Young Engineer Award. He is a Member of the Institute of Electrical and Electronics Engineers (IEEE) of USA, the Optical Society of America(OSA) of USA, the Institute of Electronics, Information, and Communication Engineers (IEICE) of Japan, and the Society of Information Theory and Its Applications (SITA) of Japan.



Iwao Sasase was born in Osaka, Japan, in 1956. He received the B.E., M.E., and Ph.D. degrees in electrical engineering from Keio University, Yokohama, Japan, in 1979, 1981, and 1984, respectively. From 1984 to 1986, he was a Postdoctoral Fellow at the University of Ottawa, Ottawa, ON, Canada. He is now a Professor of Information and Computer Science at Keio University. His research interests include modulation and coding, mobile communications, satellite communications, optical communications, communication networks, and information theory. He has published more than 250 journal papers and 361 international conference papers.

He received 1984 IEEE Communication Society Student Paper Award (Region 10), 1986 Inoue Research Award, 1988 Hiroshi Ando Memorial Young Engineer Award, and 1996 IEICE Switching System Technical Group Best Paper Award. He is a Senior Member of the Institute of Electrical and Electronics Engineers (IEEE) of USA, a Member of the Institute of Electronics, Information, and Communication Engineers (IEICE) of Japan, the Information Processing Society of Japan, and the Society of Information Theory and Its Applications (SITA), Japan. He served as the Director of the IEEE ComSoc Asia Pacific Region (2004–2005), the Chair of the IEEE ComSoc Satellite and Space Communications Technical Committee (2000–2002), the Vice President of the IEICE Communications Society (2004–2006), the Chair of the IEICE Network System Technical Committee (2004–2006), the Chair of the IEICE Communication System Technical Committee (2002–2004), and Director of the Society of Information Theory and Its Applications in Japan (2001–2002).